TISSUE ENGINEERING: Part C
Volume 24, Number 2, 2018

DOI: 10.1089/ten.tec.2017.0342

termis
Tissue Engineering
& Regenerative Medicine
International Society

METHODS ARTICLE

A Miniature Swine Model for Stem Cell-Based *De Novo* Regeneration of Dental Pulp and Dentin-Like Tissue

Xiaofei Zhu, DDS, PhD,[1,2] Jie Liu, DDS, PhD,[1] Zongdong Yu, MD, MS,[1] Chao-An Chen, DDS, MS,[1,3] Hacer Aksel, DDS, PhD,[1,4] Adham A. Azim, BDS,[1,*] and George T.-J. Huang, DDS, MSD, DSc[1]

The goal of this study was to establish mini-swine as a large animal model for stem cell-based pulp regeneration studies. Swine dental pulp stem cells (sDPSCs) were isolated from mini-swine and characterized *in vitro*. For *in vivo* studies, we first employed both ectopic and semi-orthotopic study models using severe combined immunodeficiency mice. One is hydroxyapatite-tricalcium phosphate (HA/TCP) model for pulp-dentin complex formation, and the other is tooth fragment model for complete pulp regeneration with new dentin depositing along the canal walls. We found that sDPSCs are similar to their human counterparts exhibiting mesenchymal stem cell characteristics with ability to form colony forming unit-fibroblastic and odontogenic differentiation potential. sDPSCs formed pulp-dentin complex in the HA/TCP model and showed pulp regeneration capacity in the tooth fragment model. We then tested orthotopic pulp regeneration on mini-swine including the use of multi-rooted teeth. Using autologous sDPSCs carried by hydrogel and transplanted into the mini-swine root canal space, we observed regeneration of vascularized pulp-like tissue with a layer of newly deposited dentin-like (rD) tissue or osteodentin along the canal walls. In some cases, dentin bridge-like structure was observed. Immunohistochemical analysis detected the expression of nestin, dentin sialophosphoprotein, dentin matrix protein 1, and bone sialoprotein in odontoblast-like cells lining against the produced rD. We also tested the use of allogeneic sDPSCs for the same procedures. Similar findings were observed in allogeneic transplantation. This study is the first to show an establishment of mini-swine as a suitable large animal model utilizing multi-rooted teeth for further cell-based pulp regeneration studies.

Keywords: dental pulp stem cells, mini-swine, pulp regeneration, ectopic model, tooth fragment model, orthotopic model, autologous, allogeneic

Introduction

Significant progress has been made in the past decade on stem cell-based approach in pulp-dentin regeneration using various animal study models. Using a tooth slice or tooth fragment model transplanted in the subcutaneous space of immunocompromised mice, such a semi-orthotopic approach has demonstrated *de novo* pulp regeneration with newly formed dentin-like mineral deposits on the canal wall by the implanted human dental pulp stem cells (DPSCs).[1,2] There are several advantages of this mouse model: (1) human DPSCs were used without the concern of rejection because of the mouse immunocompromised condition; (2) it is easy to perform experiments on the subcutaneous space of small animals; and (3) the tooth samples used provide an orthotopic-like environment and space for pulp and dentin regeneration to take place, especially the tooth fragment design. There are, however, obvious disadvantages of such mouse models: (1) the blood supplies in the mouse subcutaneous tissues is very different from periapical tissues; (2) the operating procedures for pulp-dentin regeneration on the tooth samples is very different from working in the clinic; and (3) the regenerated tissues are produced and populated by both human and mouse cells.

Orthotopic *de novo* pulp regeneration was demonstrated in a dog model by Iohara *et al.* using autologous subpopulation of $CD105^+$ DPSCs.[3] The regenerated pulp was well vascularized and innervated. Subsequently, the same research team

[1]Department of Bioscience Research, College of Dentistry, University of Tennessee Health Science Center, Memphis, Tennessee.
[2]VIP Dental Service and Geriatric Dentistry, School and Hospital of Stomatology, Peking University, Beijing, China.
[3]Department of Endodontics, Chi Mei Medical Center, Liouying, Tainan, Taiwan.
[4]Department of Endodontics, School of Dentistry, Hacettepe University, Ankara, Turkey.
**Current affiliation:* Department of Periodontics & Endodontics, School of Dental Medicine, University at Buffalo, Buffalo, New York.

utilized various cell populations and approaches to further confirm the success of *de novo* pulp regeneration in the dog model.[4,5] Other reports using cell-based pulp regeneration approach along with the use of platelet-rich plasma in the dog model, however, did not demonstrate pulp regeneration[6,7] while only periodontal and bone tissues were identified in the pulp space.[8]

Miniature swine has been utilized as a large animal study model in multiple fields of biomedical research for their similarity to humans anatomically, physiologically, or genetically.[9,10] Using miniature swine for dental research has also long been recognized and various types of dental and oral research including pulp capping for dentinogenesis and repairing mandibular bony defect have used mini-swine as a suitable study model.[11–18] Thus, the purpose of this study was to test and establish miniature swine as a large animal model to study orthotopic stem cell-based pulp and dentin regeneration including the use of single- and multi-rooted teeth.

We performed stepwise experimental approaches starting from *in vitro* stem cell characterization to *in vivo* ectopic, semi-orthotopic, and orthotopic tissue regeneration.

Materials and Methods

For tooth sample collection, cell cultures, flow cytometry and multi-differentiation studies, sample processing for histological examination, and immunohistochemistry, see Supplementary Data (Supplementary Data are available online at www.liebertpub.com/tec).

Ectopic pulp-dentin complex formation mouse model

This mouse model utilizes hydroxyapatite/tri-calcium phosphate hydroxyapatite (HA/TCP) granules (Berkeley Advanced Biomaterials, Inc., Berkeley, CA) as the key material based on previous studies.[19,20] In brief, over-confluent cells (2 days after confluence) were harvested and mixed with HA/TCP and incubated with rotation for 90 min at 37°C. The mixture (4×10^6 cells/40 mg HA/TCP) was then transplanted subcutaneously into the back of a NOD.CB17-Prkdcscid/J mouse (female, ~7 weeks old) (Jackson Labs., Bar Harbor, Maine). Two-three months later the mice were euthanized and transplants harvested for histological and/or immunohistochemical analysis. All mouse procedures followed protocols approved by IACUC at BU (#AN-15027.2009.10) and UTHSC (#12-105.0-A, #15-069-A).

Semi-orthotopic tooth fragment mouse model

Previously, we established this tooth fragment model, which is semi-orthotopic for pulp regeneration because the regeneration takes place inside of a real tooth, although the tooth fragment is implanted into an ectopic location using severe combined immunodeficient (SCID) mice.[2]

Preparation of tooth fragments of human and swine teeth. Human or swine teeth were prepared into segments of ~6–10 mm in length with the root canal space enlarged to ~1 mm in diameter. Tooth fragments were then sterilized according to our published report.[2] Coronal end of the canal was sealed with mineral trioxide aggregate (MTA) cement (ProRoot MTA, Dentsply, York, PA) ~1 mm into the space. In our previous studies, MTA was applied and allowed to set under moist condition before the tooth fragment was sterilized.[2]

To simulate orthotopic regeneration in mini-swine, we first tested the approach of adding freshly mixed MTA onto the coronal end of the tooth fragment after the canal was injected and filled with cells/scaffold mixture (scaffold materials described in below sections), followed by immediate transplantation into the mice. However, we found that the unset MTA rendered animals ill. We suspected that the high pH of MTA during the early phase of setting may cause damage and the relative amount of MTA in proportion to mice was too large. Thus, we went back to the previous protocol by having the set MTA on the tooth fragments before cell injection and *in vivo* transplantation.

Insertion of cells/scaffolds into tooth fragments and implantation into mouse subcutaneous space. Cells were carried by one of the two scaffold systems. For poly-D,L-lactide/glycolide (PLG) scaffold, it was originally made into 5 (diameter)×2 (height) mm solid porous discs with pore diameters of 250–425 μm as described previously.[2] The PLG disc was cut into pieces (≤1 mm^3 apiece) and seeded with ~10^7 cells/mL, which were then inserted into the canal space.[2]

For injectable gel, cross-linked hyaluronic acid (HyA) gel (24 mg/mL) (Juvederm-ultra; Allergan, Inc., Irvine, CA) was mixed with cells (resuspended in medium containing HEPES 25 mM) at 1:1–1:1.4 (v/v, i.e., gel/cells) ratio with final cell concentration of ~2×10^7/mL. Regarding cell/gel mixing, we first used pipetting and found that 1:1.4 (gel:cells) ratio was needed to mix well as the gel was very viscous. Later, we identified a mixing process involving a modified syringe-to-syringe mixing/delivery system (Ultradent Product, Inc., South Jordan, UT) in which two syringes connected at the front end. The Ultradent syringe was first sterilized by soaking in ~3% NaOCl for a few days and rinsed with sterile PBS before using.

The Ultradent syringe received HyA gel and the other 1-mL sterile syringe contained resuspended cells. The syringe plunger was then pushed slowly from one syringe to deliver the gel or cells into the other syringe, followed by pushing back from the other syringe plunger for a total of at least 10 times to mix the cells and gel. The 1-mL syringes eventually collected all

FIG. 1. Isolation of swine dental stem cells. **(A)** Initial formation of colonies within 1–2 weeks after isolation from tissues. Scale bar: 300 μm for all four images. **(B)** Cells at passage 1 seeded sparsely onto 6 cm dishes forming individual CFU-Fs. Cells were fixed and stained with 0.5% *crystal violet* in methanol. **(C)** Flow cytometry analysis of mini-swine DPSC cell surface markers. **(D, E)** Odonto-differentiation showing Alizarin red staining after 5 weeks of osteogenic stimulation. Representative cell culture images are from scanned images of wells of 12-well plates and microscopic images (scale bar: 500 μm for all four microscopic images). **(F, G)** Adipogenic differentiation of sDPSCs and sSCAP after 56 days of stimulation and cultures stained with Oil Red O. No staining was observed. Representative cell culture images are from scanned images of wells of 12-well plates and microscopic images (scale bar: 500 μm for all four microscopic images). CFU-F, colony formation units of fibroblastic cell; sDPSC, swine dental pulp stem cell; sSCAP, swine stem cells of apical papilla.

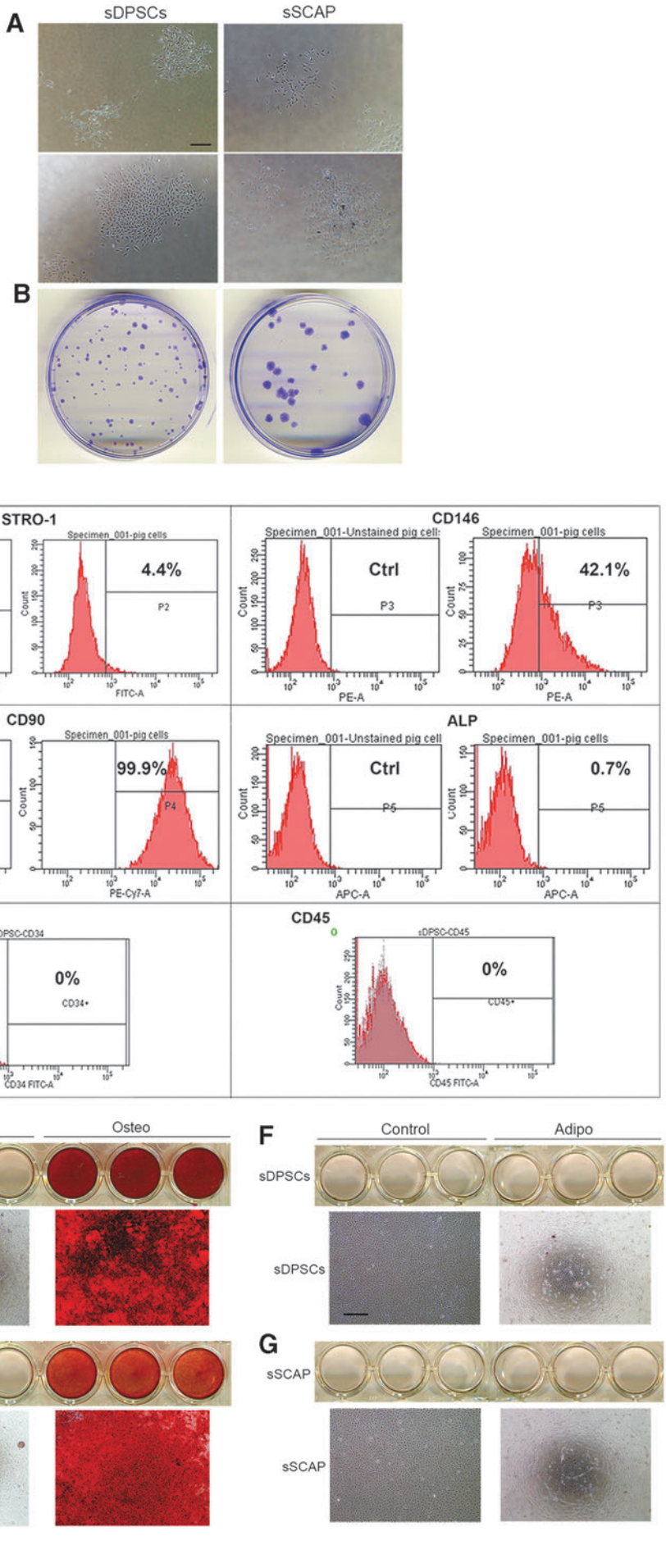
A
sDPSCs
sSCAP
B
C
STRO-1
Specimen_001-Unstained pig cells
Specimen_001-pig cells
Ctrl
4.4%
P2
FITC-A
CD146
Specimen_001-Unstained pig cell
Specimen_001-pig cells
Ctrl
42.1%
P3
PE-A
CD90
Specimen_001-Unstained pig cells
Specimen_001-pig cells
Ctrl
99.9%
P4
PE-Cy7-A
ALP
Specimen_001-Unstained pig cell
Specimen_001-pig cells
Ctrl
0.7%
P5
APC-A
CD34
sDPSC-CD34
0%
CD34+
CD34 FITC-A
CD45
sDPSC-CD45
0%
CD45+
CD45 FITC-A
Count
D
Control
Osteo
sDPSCs
sDPSCs
E
sSCAP
sSCAP
F
Control
Adipo
sDPSCs
sDPSCs
G
sSCAP
sSCAP

the mixed cells/gel, the front end was then disconnected from the other syringe and replaced with a 23–25 gauge needle for delivery of the cells/gel mixture into the root canal space.

All steps were performed in a tissue culture hood using sterile techniques. The tooth constructs were then transplanted into the subcutaneous space on the back of 6–8-week old female SCID mice (NOD.CB17-*Prkdc-scid*/J). Three months later, mice were euthanized and tooth fragments removed for histological analysis. All animal procedures followed protocols approved by the IACUC, as mentioned above.

Orthotopic mini-swine model

Approximately, 14-month-old female Sinclair or Yucatan miniature swine were used (Sinclair-BioResources, LLC Auxvasse, MO; ~14-month-old; $n=5$). All operations on mini-swine were performed under general anesthesia beginning with telazol (4–6 mg/kg) and maintained with isoflurane. Preoperative X-rays were taken and the four canines were extracted to isolate dental stem cells (DSCs). All tooth operations were preceded by cleaning the teeth with ultrasonic tips to remove dental plague and disinfection with betadine and 6% NaOCl. When cells were ready for transplantation animals were anesthetized, teeth were cleaned and isolated by rubber dam. After pulp exposure, working lengths were established by X-rays followed by rotary NiTi files to remove pulp and enlarge canals with the apex opened to at least #45. Canals were irrigated with 1.5% NaOCl followed by 17% EDTA and normal saline.

After canals were dried with sterile paper points, autologous or allogeneic sDPSCs ($\sim 2\times10^7$/mL) mixed with HyA gel (24 mg/mL) or Collagen TE gel (ColTE; 5.4 mg/mL. Nitta Gelatin, Inc., Osaka, Japan)[3] were delivered into the canals via a 1-mL syringe with 25 gauge needle long enough to reach the apical third. Subsequently, CollaCote or HA/TCP was placed over the orifices, and MTA cement followed by light cure composite resin bonding were used to seal the tooth. In general, one quadrant of teeth were operated in each operation that required ~5 h. The animals were sacrificed 1.5–4 months later, and the teeth were sectioned into blocks or extracted for further processing described below.

Results

In vitro *characterization of swine DSCs*

Isolated swine heterogeneous population of sDPSCs and stem cells of apical papilla (sSCAP) emerged in cultures showing typical mesenchymal stem/progenitor cell (MSC) characteristics with colony formation units of fibroblastic cells (Fig. 1A, B). We examined heterogeneous sDPSC surface MSC markers by flow cytometry and they showed 4.4% STRO-1, 42.1% CD146, 99.9% CD90, and 0.7% ALP-positive cells in the population, while CD34 and CD45 were negative (Fig. 1C).

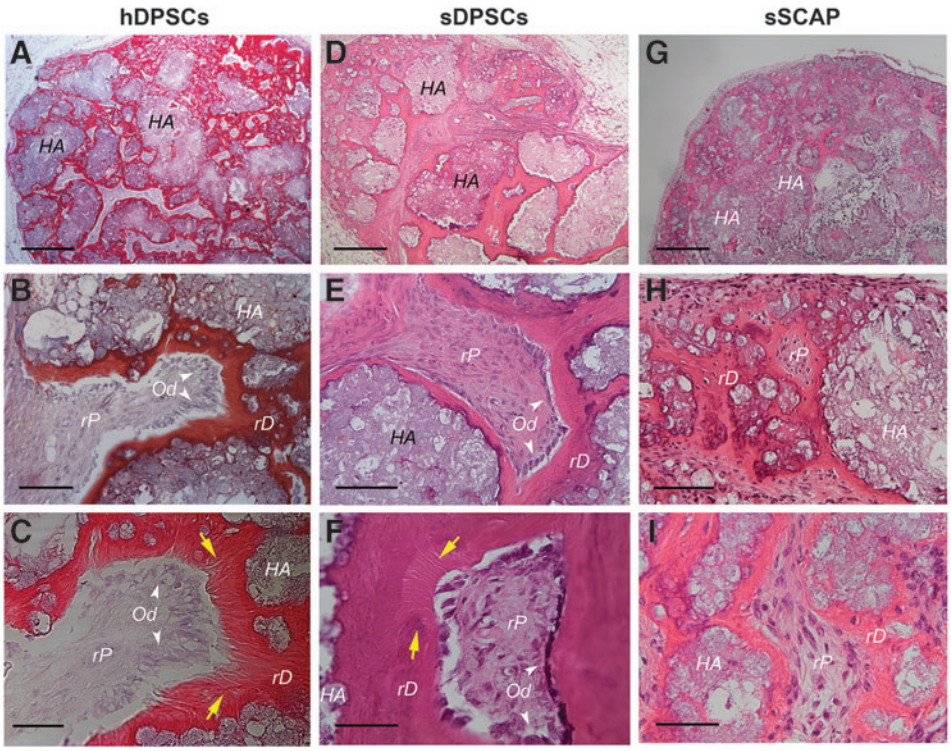

FIG. 2. *In vivo* formation of ectopic pulp-dentin complex. Dental stem cells (passage 3) were mixed with HA/TCP and transplanted into SCID mice. Samples were harvested after 2 (sSCAP and hDPSCs) to 3 (sDPSCs) months and processed for H&E analysis. **(A–C)** hDPSCs formed mineral tissues (*pink, red*) with connective soft tissue resembling pulp. At higher magnifications **(B, C)**, Odontoblast-like cells (Od) that produced the minerals are indicated by *white arrowheads*. Dentinal tubule-like structures extending from the Od side into the mineral tissue are indicated by the *yellow arrows* **(C)**. **(D–F)** pulp-dentin complex formed by sDPSCs. Od lining against the mineral tissue and dentinal tubule-like structures are indicated (*yellow arrows*). **(G–I)** sSCAP formation of pulp-dentin complex. No obvious Od lining against the mineral tissue, nor are there dentinal tubule-like structures observed. HA: hydroxyapatite/tri-calcium phosphate; rD: dentin-like; rP: pulp-like. Scale bars, *Top* three images: 500 μm; *middle* three: 100 μm; *bottom* three: 50 μm. HA/TCP, hydroxyapatite-tricalcium phosphate.

sDPSCs and sSCAP were highly odontogenic with considerable amounts of mineral deposits in cultures revealed by Alizarin red stain (Fig. 1D, E), whereas no adipocyte-like cells were observed by the Oil Red stain (Fig. 1F, G).

Compared to human's counterparts, sDPSCs and sSCAP appeared to be less elongated or spindle-shaped while squarer in the cell body shape. Representative images of sDPSCs and hDPSCs are shown in Supplementary Figure S1A. Under neurogenic stimulus, cells underwent morphologic changes resembling neural cells (Supplementary Fig. S1B).

In vivo *ectopic pulp-dentin complex formation*

To verify that sDPSCs and sSCAP are capable of regenerating tissues *in vivo*, standard assays using HA/TCP in a subcutaneous mouse model were performed as described previously.[19,21] We observed pulp-dentin complex formation, which was similar to those formed with the use of human counterparts (Fig. 2). We found dentin-like mineral or regenerated dentin-like (rD) mineral deposited on the surface of HA/TCP granules. The soft connective tissue adjacent to the dentin-like mineral resembled pulp, i.e., regenerated pulp-like (rP) tissue. The odontoblast-like cells were normally found lining against the rD. At higher magnifications, we noticed obvious dentinal tubule-like structures (pointed by the yellow arrows in Fig. 2C, F) especially in samples of hDPSCs and sDPSCs.

Our immunohistochemical analysis on tissues regenerated by hDPSCs and sDPSCs revealed that odontoblast-like cells that lined against the rD and some cells in the rP area expressed nestin, DSP, DMP1, and BSP (Fig. 3). Some odontoblast-like cells showed polarized cell bodies (Fig. 3, sDPSC panel, blue arrow) and rD structure contained dentinal tubule-like structures (Fig. 3, yellow arrows). BSP expression appeared relatively weak compared to nestin and DSP. Faint staining of DSP and DMP1 may also be located on some dentin-like mineral. Antibody specific to human mitochondria detected positively stained cells in samples of hDPSCs. Isotype control antibodies did not react to those antigens (Supplementary Fig. S2).

Semi-orthotopic regeneration in vivo *using tooth fragment mouse model*

We have previously demonstrated that if the tooth fragment apical opening is large (~2–3 mm in diameter), canal is wide and the tooth is short, transplanted DPSCs or SCAP loaded on the small pieces of PLG (poly-D,L-lactide & glycolide) scaffold (~1–2 mm^3) in the canal space may survive well and pulp regeneration can occur in the entire canal space with a layer of rD on the canal walls and below the MTA.[2] However, when longer tooth fragment with small apical openings (≤1 mm) were used, the cell-based pulp regeneration in the mouse model did not work well as many

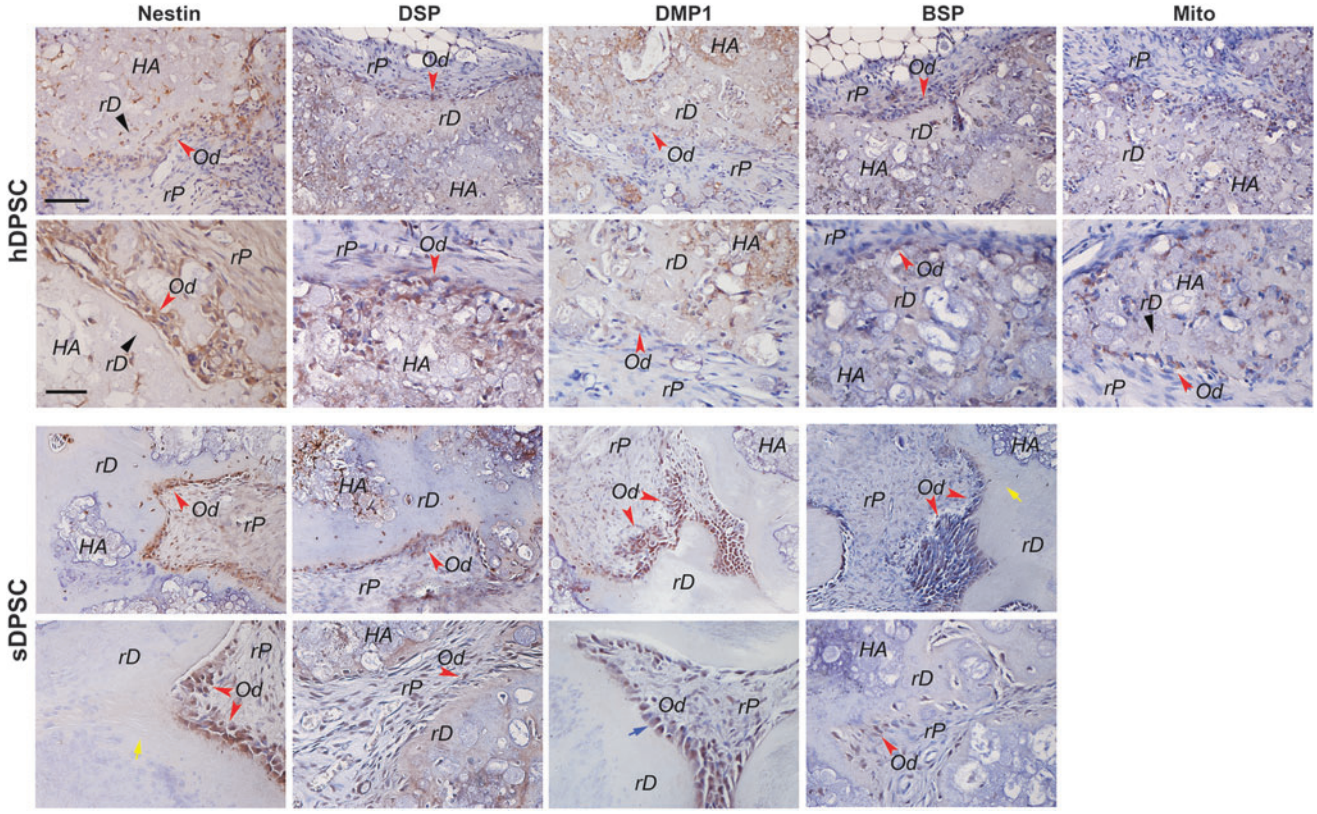

FIG. 3. Immunohistochemical analysis of *in vivo* formation of ectopic pulp-dentin complex. Dental stem cells were mixed with HA/TCP and transplanted into SCID mice. Samples were harvested after 2–3 months and processed for analysis. Specific antibodies against human nestin, DSP, and DMP-1. BSP and mitochondria were used to detect these gene products in tissues formed by either hDPSCs or sDPSCs. Positive staining is shown by *brown* stains mainly in individual cells and some mineral tissue (weakly). *Black arrowheads*: rD; *red arrowheads*: Od (odontoblast-like); *yellow arrows*: dentinal tubule-like; blue arrow: polarized odontoblast-like cells. Scale bars: for *top panels* of both hDPSCs and sDPSCs, 100 μm; *Bottom panels* for both cell types, 50 μm.

samples showed little pulp regeneration and only near apex (Supplementary Fig. S3). Also, the PLG packing was difficult to control in longer roots causing the PLG being compressed and therefore placing highly condensed PLG scaffold in the canal space, which prevented pulp regeneration to occur (Supplementary Fig. S3B).

We then decided to change to cross-linked HyA gel as a cell carrier and scaffold, which has been used clinically for cosmetic purpose, that is, it has been tested to be safe for human medical applications. As shown in Supplementary Figure S4, a sample with the MTA dislodged after transplantation allowing the blood supply enter the canal from both coronal and apical ends. This resulted in a complete regeneration of pulp in the long canal space (~8 mm) with only ~1 mm apex opening. In this sample, only a layer of dense connective tissue deposited along the dentin wall was observed, likely a longer time was needed to allow calcification. At higher magnifications, we observed the depositing dense fibrous projection into the existing dentinal tubules, indicating that the tubular space may become filled with these newly generated fibers by these pulp cells or odontoblast-like cells (Supplementary Fig. S4F).

For samples that the coronal end was well sealed and the apex was only ≤1 mm opening, the regeneration was inconsistent. In most cases, the pulp regeneration only reached to middle or apical third of the canal (9 of 13 samples), and some had no tissue or only fat tissue from the mouse subcutaneous

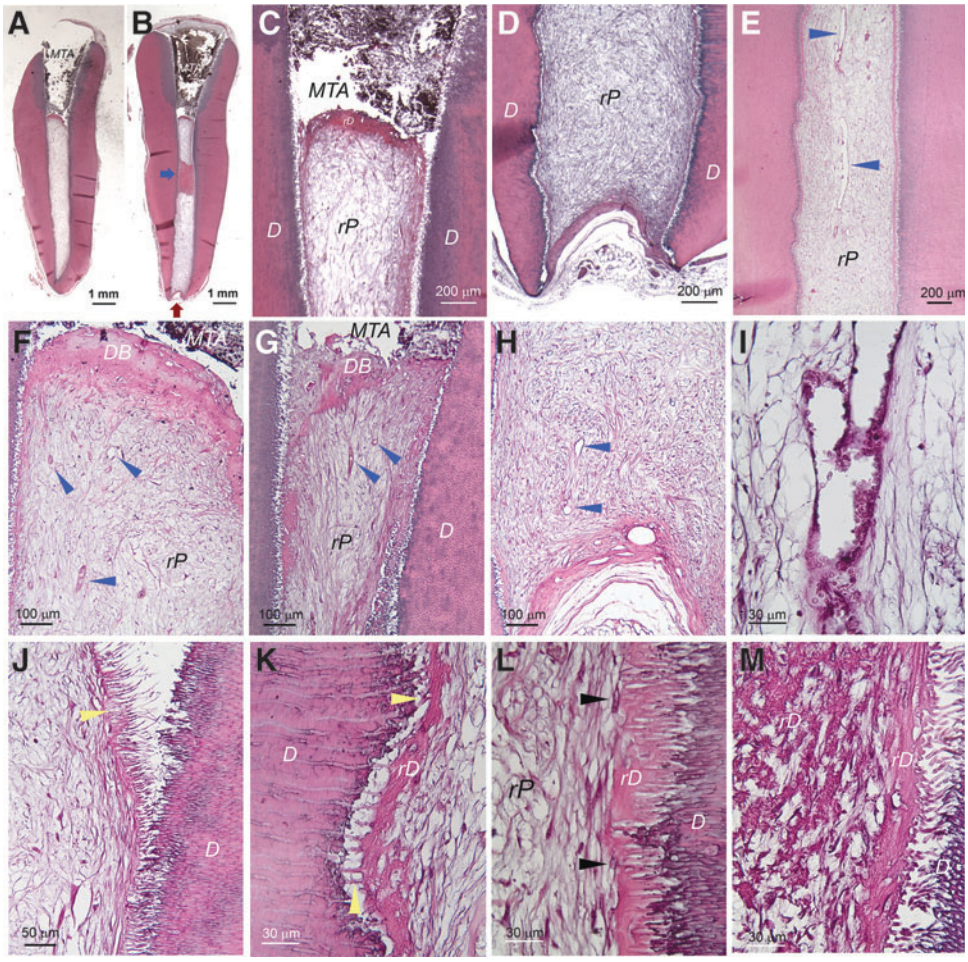

FIG. 4. Histological analysis of pulp regeneration in human tooth fragment model. hSCAP (passage 2) mixed with HyA were injected into canal space of tooth fragment and transplanted into the subcutaneous space of SCID mice. After 3 months, the tooth fragment was retrieved and processed for histology. **(A, B)** Full view of the tooth fragment showing MTA filling on the coronal end allowing blood supply to enter the canal only from the apex [*red arrows* in **(B)**]. *Blue arrow* in **(B)** showing rD on the canal wall at the sectional plane due to elevation of that part of the canal wall into the canal space. **(C, D)** Closer views of the coronal and apical areas of the sample. **(E)** Mid-root area of the canal space showing well vascularized (*blue arrowheads*) regenerated pulp-like tissue (rP). **(F, G)** Coronal areas of two different sections showing regenerated dentin-like bridge (DB) underneath the MTA. *Blue arrowheads* showing many blood vessels under the DB. **(H)** Apical region showing substantial vascularization (*blue arrowheads*) near apical opening. **(I)** Higher magnification showing the blood vessel and the loose connective tissue formation in pulp space. **(J)** Near coronal area showing dense fibers along the canal wall (*yellow arrowhead*). The fibers show brush-like morphology. They were separated from the canal wall and dentinal tubules during the sample processing. **(K, L)** Higher magnification showing regenerated dentin-like (rD) mineral tissue deposited along the canal wall. *Yellow arrowheads* pointing at the fibers extending into the existing dentinal tubules. The *black arrowheads* in **(L)** pointing at the cells along the rD that may be involved in generating mineral rD. **(M)** Higher magnification showing the area indicated by the *blue arrow* in **(B)**. Crystal-like structures indicating possibility of calcified fibrous bundles of rD.

space in the canal (3 of 13 samples). As an example having pulp-like tissue regeneration only in apical third of the canal is presented in Supplementary Figure S5. The coronal half/third of the canal showed only low quality loose connective tissues or amorphous materials that were often lost during specimen processing. A sample of complete pulp regeneration (1 of 13 samples) in a narrow long canal (~8 mm) with a small apex opening (<1 mm) is shown in Figure 4. Dentin-like bridge (DB) under the MTA was formed (Fig. 4A–C, F, G) and good vascularity was shown throughout the rP (Fig. 4E–I). In terms of the density of the rP (Fig. 4I), it seemed low compared to normal pulp, possibly requiring longer time to produce denser soft tissue. At higher magnifications, we observed a thin layer of rD or osteodentin deposited onto the dentin walls (Fig. 4J–L). It appeared that the newly deposited rD filled into the dentinal tubules (Fig. 4J, K). Cells lining against the rD were flat

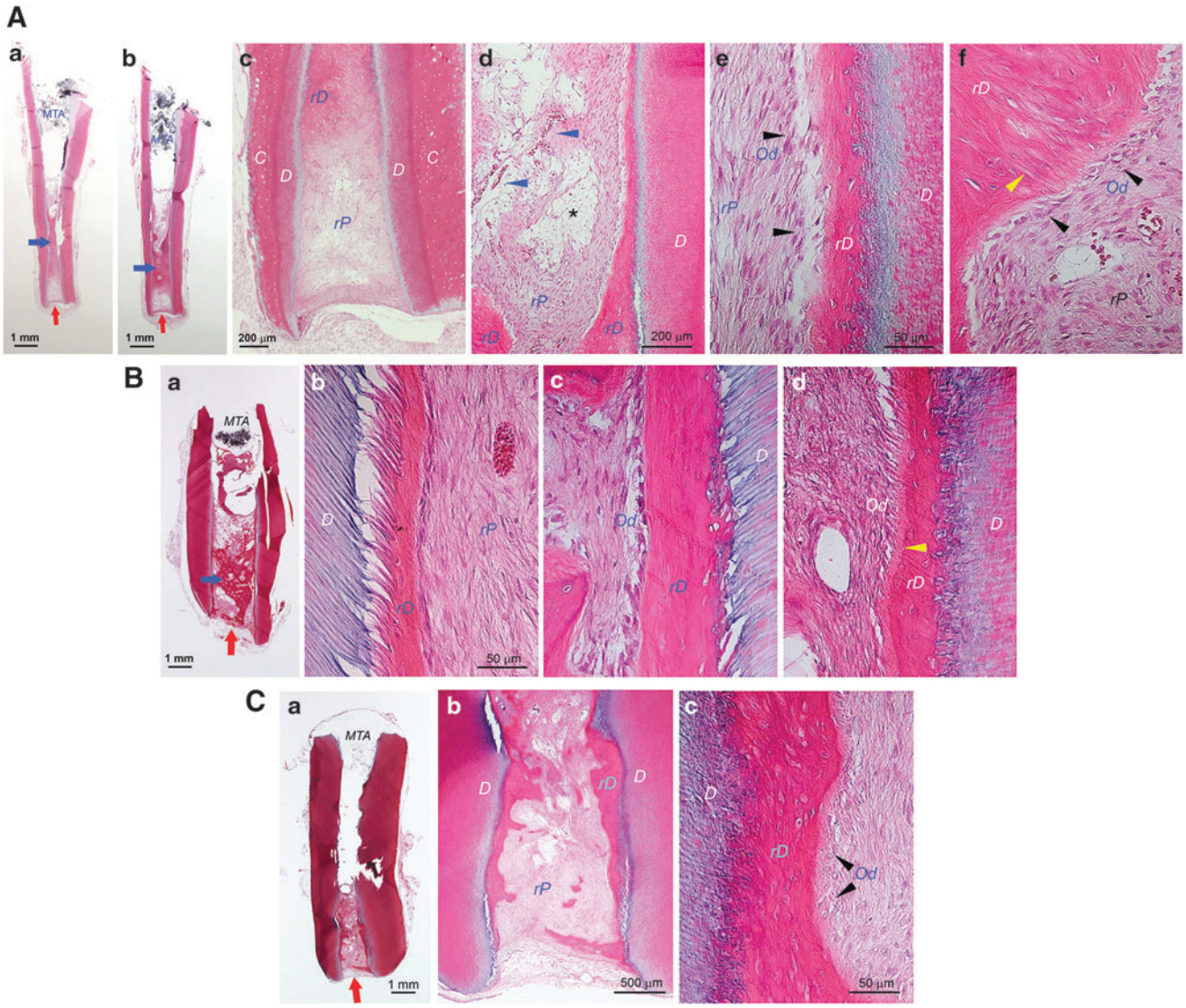

FIG. 5. Histological analysis of pulp regeneration in swine tooth fragment model. sDPSCs or sSCAP mixed with HyA were injected into the canal space of swine tooth fragment and transplanted into the subcutaneous space of SCID mice. After 3 months, the tooth fragment was retrieved and processed for histology. **(A)** sDPSCs at passage 0 were used. **(Aa, b)** Full view of the tooth fragment showing lacking tissue in the coronal half of the canal. **(Ac)** Closer view showing apical areas of the canal with regenerated pulp-like (rP) tissue but lacking additional dentin-like tissue on the dental wall (D). C: cementum. **(Ad)** Mid-root area of the canal space showing well vascularized (*blue arrowheads*) rP. *Sign indicates the area of rP is loose, possibly caused by the remaining HyA. **(Ae, f)** Higher magnification (scale bar: 50 μm for both images) showing odontoblast-like cells (Od, *black arrowheads*) producing regenerated osteodentin (rD). *Yellow arrowhead* pointing at dentinal tubule-like structure in the rD shown in **(Af)**. **(B)** sSCAP at passage 3 were used for the experiment. **(Ba)** Full view of the tooth fragment showing coronal half does not contain well regenerated tissues. **(Bb–d)** Higher magnification (scale bar: 50 μm for all three images) showing rP, rD and Od. *Yellow arrowhead* in **(Bd)** showing predentin-like tissue with less intensity of eosin stain. **(C)** sSCAP at passage 3 were used for the experiment. **(Ca)** Full view of the tooth fragment showing coronal absent of tissues. **(Cb, c)** Higher magnification showing rP, rD and Od. Note: **(Aa, b; Ba; Ca)** are full view of the tooth fragment showing MTA filling on the coronal end allowing the blood supply to enter the canal only from the apex (*red arrows*). *Blue arrows* in **(Aa, b)** and **(Ba)** indicate the rD on the canal wall at the sectional plane due to the elevation or angulation of that part of the wall into the canal space.

fibroblast-like lacking the odontoblast-like characteristics (Fig. 4L). At closer examination of the area where rD on the canal wall is revealed at the sectional plane due to the elevation of that part of the wall into the canal space, we observed crystal-like microstructure, likely representing the calcifying collagen fibers (Fig. 4M).

Swine tooth fragments and cells were used for this *in vivo* model the same way as for the human system. As demonstrated in Figure 5, swine cells transplanted into swine teeth also showed formation of regenerated pulp. Similar to the human system, coronal tissue regeneration was absent or in poor quality, which may have been lost during sample processing. Nonetheless, in the apical area where rP formation occurred, we observed vascularity and the deposition of rD containing embedded cells on the root canal dentin walls. The rD projected or extended into the canal space in some region of the canal. This made the pulp look like having filled with calcifying mineral while it was not. Some odontoblast-like cells along the rD did appear ovoid or columnar in shape resembling natural odontoblasts (Fig. 5Ae, f; Bc; Cc). Although we did not observe dentinal tubules in the rD in general, some regions of the rD did demonstrate formation of dentinal tubule-like structure (Fig. 5Af, yellow arrowhead). Additionally, we observed some regions showing predentin-like appearance in the rD (Fig. 5Bd, yellow arrowhead).

Orthotopic pulp regeneration in mini-swine

After confirming the pulp regeneration using swine cells in the mouse model, we moved onto the orthotopic model focusing on only sDPSCs as pulp tissue was more easily accessible than apical papilla. Natural pulp tissue of mini-swine was first examined showing highly vascularized pulp and typical odontoblast layer (Supplementary Fig. S6)

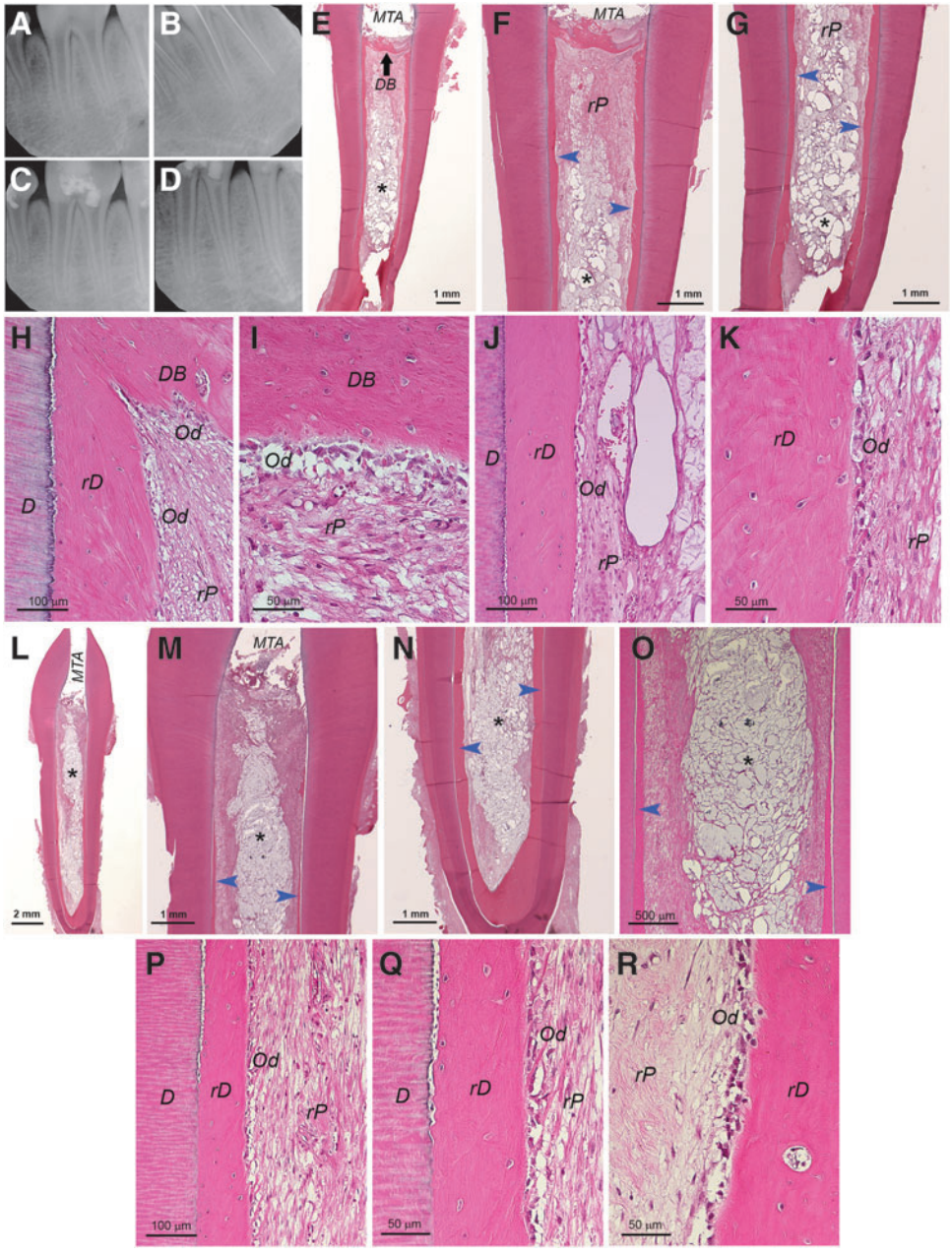

FIG. 6. Histological analysis of orthotopic *de novo* pulp regeneration in mini-swine. **(A–D)** Radiographs of a female Yucatan mini-swine mandibular *left* third premolar receiving pulpectomy, canal enlargement and autologous cell transplantation. **(A)** Preop; **(B)** during pulpectomy checking the working lengths (~21 mm); **(C)** after injection of sDPSCs (passage 2) mixed with HyA into the canals, the tooth was sealed with MTA and bonding composite; **(D)** ~3 months later at sacrifice. **(E)** Full view of the distal root showing root canal space filled with tissue. *Black arrow* indicates dentin bridge-like (DB) mineral tissue formation underneath the HA/TCP+MTA. **(F, G)** Closer view of the coronal **(F)** and apical **(G)** half of the sample showing regenerated dentin-like (rD) mineral formation on the existing dentin walls (*blue arrowheads*). **(H–K)** Higher magnification views of rD, DB, rP, odontoblast-like cells (Od). **(L)** Full view of the mesial root showing pulp regeneration. **(M, N)** Closer view of the coronal **(M)** and apical **(N)** half of the sample showing rD (*blue arrowheads*). **(O)** Closer view of the mid-root area showing rD. **(P–R)** Higher magnification views of rD, DB, rP and Od. Note: *Sign indicates the area of rP is loose or lacking normal pulp-like tissue caused by the remaining HyA.

resembling their human counterparts. In Figure 6, we observed orthotopic pulp regeneration using autologous sDPSCs on a mandibular third premolar in which the root canal system is similar to a human molar with multiple roots. Radiographs in Figure 6A–D show working length determination and canal filling with transplanted cells. At the sacrifice (~3 month after cell transplantation), the radiograph (Fig. 6D) showed dentin bridge formation underneath the HA/TCP+MTA and mild thickening of the roots compared to the postoperative radiograph (Fig. 6C).

Upon histological exmaination of the distal root, we observed a layer of DB under HA/TCP+MTA and a newly deposited mineral along the canal walls (Fig. 6E–K). The DB appeared incomplete and contained entrapped cells. The DB in the mesial root (Fig. 6L–R) was not present in the section shown. The newly deposited mineral along the canal wall was more apparent at the mid- and apical root regions. The rP in the canal space showed some remaining HyA scaffolds yet to be resorbed and seemed more obvious in the mesial canal. At higher magnifications (Fig. 6H–K, P–R), we observed the mineral deposit rD on the canal wall containing entrapped cells and no obvious dentinal tubules present. This is similar to what was observed in the tooth fragment model. Odontoblast-like cells lining against the rD can be seen with varying morphology mostly ovoid or columnar shapes.

Another case presented in Figure 7 showing a mandicular fourth premolar receiving autologous sDPSCs mixed with ColTE for pulp regeneration. Radiographs also showed the work process (Fig. 7A–D) and there was thickening of the root at sacrifice (~4 months after cell transplantation). Histological analysis revealed formation of DB under the HA/TCP+MTA in both roots (Fig. 7E–K). The DB appeared thicker than what was observed in Figure 6, however, DB contained fissures with cells entrapped in it (Fig. 7E–G).

There was also a layer of deposited rD along the canal walls. rP appeared well vascularized up to the coronal region and the tissue quality relatively more homogeneous compared to the case shown in Figure 6 in which HyA was used. ColTE is less concentrated and easier to homogeneously mix with cells. Also, the higher concentration of HyA may take longer time to be resorbed. We have cases at 5 months and observed no remaining HyA from collected sample sections (data not shown). It also could be that the transplanted ColTE as collagen could not be easily discerned histologically.

We performed immunohistochemistry to detect nestin, DSP, DMP1, and BSP expression in the teeth. In general, as shown in Figure 8, these markers were detected mainly in the odontoblast-like cells along the rD. The rP tissue matrix appeared to show some weak staining of these markers

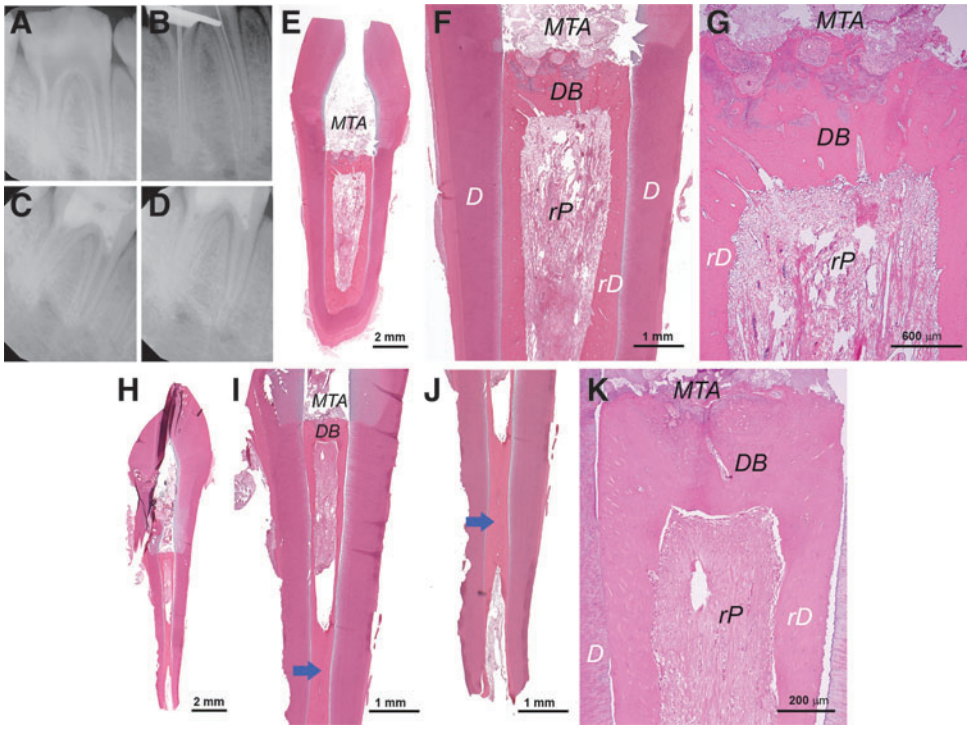

FIG. 7. Histological analysis of orthotopic *de novo* pulp regeneration in mini-swine. A female Yucatan mini-swine mandibular *right* fourth premolar receiving pulpectomy, canal enlargement and autologous cell transplantation. After ~4 months, animal was sacrificed and tooth processed for analysis. **(A)** Pre-op; **(B)** during pulpectomy checking the working lengths (~25 mm); **(C)** after injection of sDPSCs (passage 2–3)/ColTE into the canals, the tooth was sealed with MTA and bonding composite; **(D)** ~4 months later at sacrifice. **(E–G)** Mesial root. **(E)** Full view of the root. **(F, G)** Coronal section showing formation of dentin bridge-like (*DB*) mineral underneath the HA/TCP+MTA. The *DB* appears thicker than the regenerated dentin-like (*rD*) tissue along the dentin canal walls (*D*) than that in Fig. 6. Closer view image in **(G)** showing the vascularized regenerated pulp-like (*rP*) tissue and the *DB* with fissures. **(H–K)** Distal root. **(H)** Full view of the root. **(I)** Coronal half of the root showing similar formation of *DB* and *rD*. **(J)** Apical half. **(K)** Closer view showing rP, relatively thick DB under HA/TCP+MTA. Note: *Blue arrows* in **(I, J)** indicate the rD on the canal wall at the sectional plane due to the elevation or angulation of that part of the wall into the canal space.

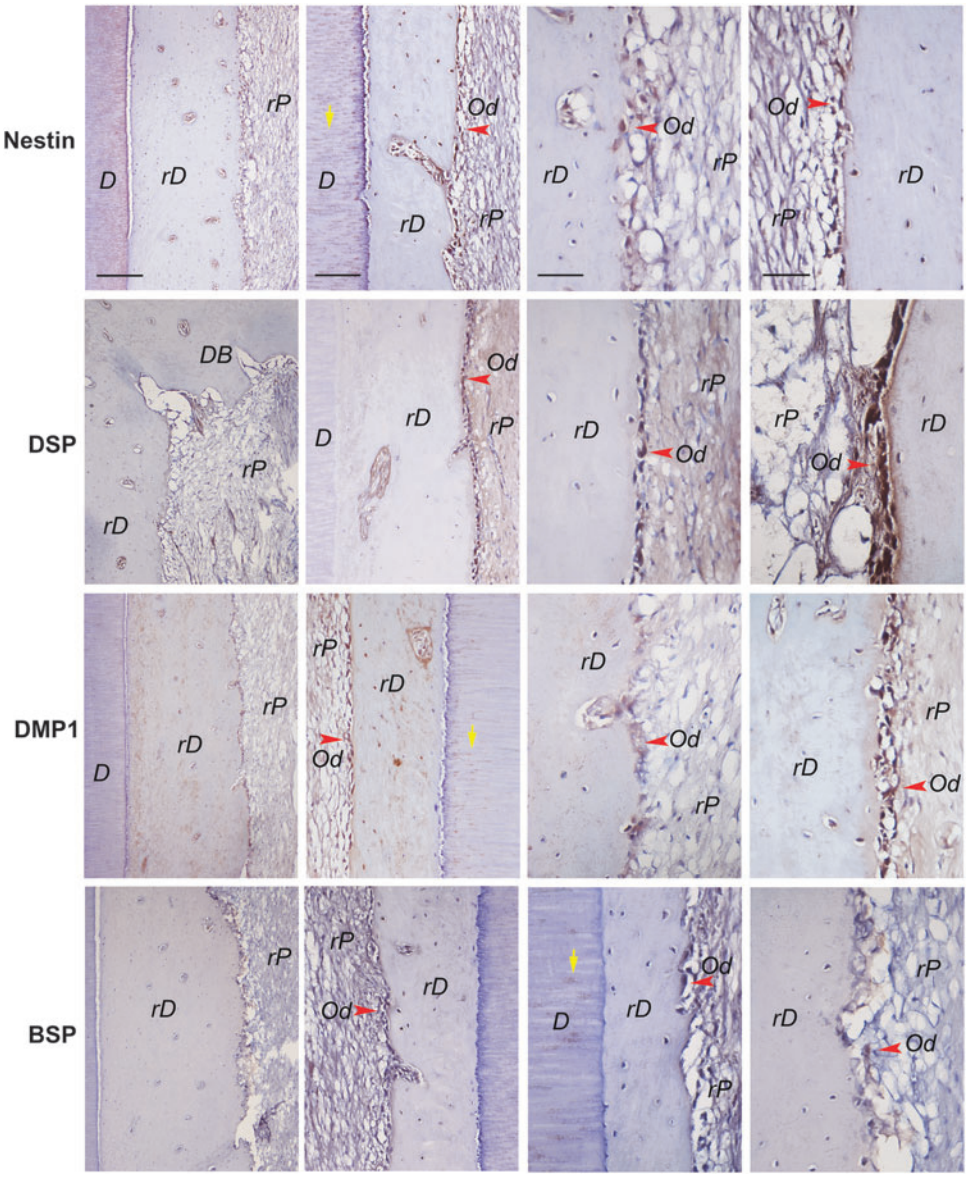

FIG. 8. Immunohistochemical analysis of orthotopic formation of pulp-dentin complex. Specific antibodies against human nestin, DSP, DMP-1, BSP were used to detect these gene products in the tissues formed by autologous sDPSCs. Positive staining is shown by *brown* stains. Samples were from regeneration experiments using either ColTE or HyA as scaffold. rD: regenerated dentin-like; rP: regenerated pulp-like; Od: odontoblast-like (*red arrowheads*); staining in dentinal tubules (*yellow arrows*) of the original dentin. Scale bars: 200 μm for images in far *left column*, 100 μm for images of *middle* and far *right columns*.

especially in areas with denser matrix formation. Nestin, DMP1, and BSP were also detected in the dentinal tubules of the original dentin. The staining was from samples that received either ColTE or HyA as scaffold for regeneration.

We also tested using allogeneic sDPSCs for pulp regeneration as shown in Figure 9 and Supplementary Figure S7. One is a mandibular third premolar receiving cells of a different breed (Yucatan to Yucatan) and the other is a mandibular second lateral incisor receiving cells of a different strain (Sinclair to Yucatan). In both cases, we observed pulp regeneration and formation of rD along the canal walls. Odontoblast-like cells lining against the rD had various morphologies from flat fibroblast-like to more ovoid in shape (Fig. 9G–I; Supplementary Fig. S7J, K). The quality of the pulp appeared suboptimal as the slow-resorbing HyA appeared to have slowed down the depositing of the pulp matrix.

In this present study, we did not observe over calcification of the pulp canal space in teeth after 5 months following cells transplantation (data not shown).

Discussion

Our present study demonstrates the first step of the establishment of mini-swine as a large animal model for orthotopic pulp regeneration studies. The tooth and root canal morphology and the overall head size of mini-swine resemble those of humans. Using such a large animal model in combination of small animal models will help experiment various conditions and troubleshoot many challenges facing pulp regeneration research. Large animal models in dental fields are in general underused for experimentation due to its technical difficulty yet in most cases a critical and an unavoidable undertaking to gather information and optimize protocols before clinical trials.

During our preliminary experiments on mini-swine, we encountered certain difficulties operating on the animals as summarized below. (1) Due to its heavy weight, the manipulation was more difficult than working on dogs compared to our previous experience.[6,7] Each post-op examination

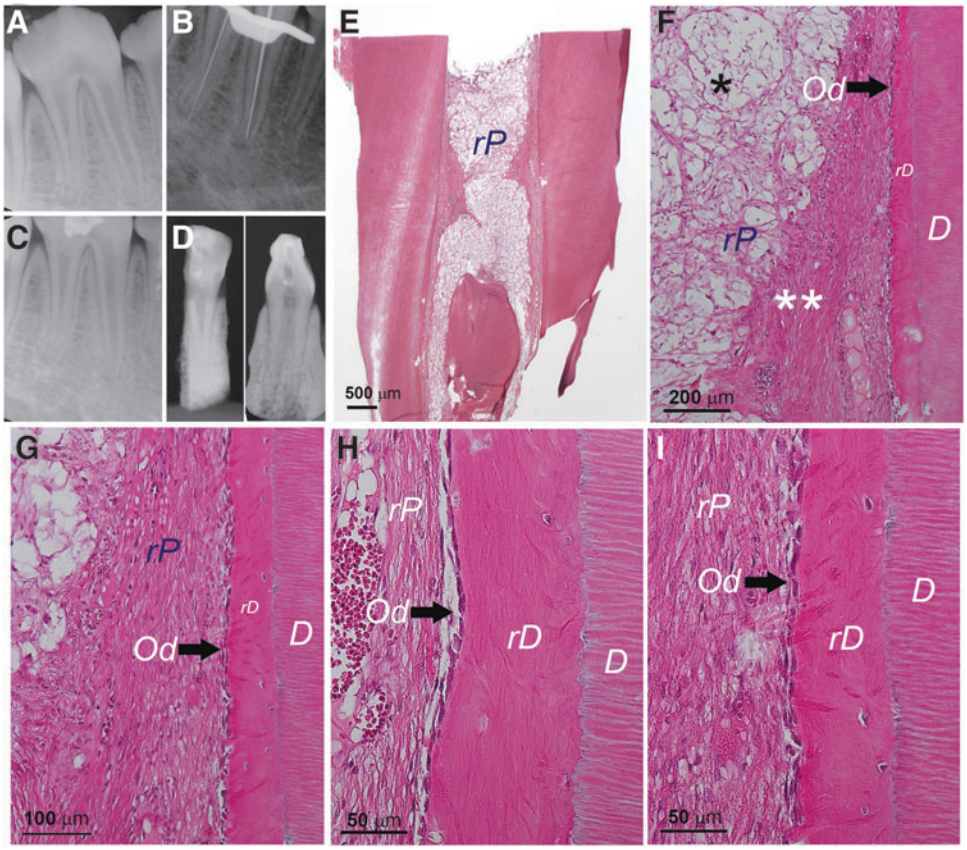

FIG. 9. Histological analysis of orthotopic *de novo* pulp regeneration in mini-swine. **(A–D)** Radiographs of a female Yucatan mini-swine mandibular *right* third premolar receiving pulpectomy, canal enlargement and allogeneic cell transplantation. **(A)** Pre-op; **(B)** during pulpectomy checking the working lengths (~20 mm); **(C)** after injection of DPSCs (passage 3)/HyA into the canals, the tooth was sealed with MTA and bonding composite; **(D)** ~6 weeks later at sacrifice showing tooth block (*Left*, buccal-lingual view; *Right*, mesial-distal view). **(E)** Longitudinal view of the mesial root showing root canal space filled with rP tissue. **(F)** Closer view of the coronal area of the sample showing regenerated dentin-like (rD) mineral formation on the existing dentin walls (D) and odontoblast-like cells (Od) (*black arrow*). **(G–I)** Higher magnification views of rD, DB, rP and Od. Note: *Sign indicates the area of rP is loose or lacking normal pulp-like tissue caused by the remaining HyA. **denser soft tissue similar to normal pulp.

required sedation. (2) Tooth sample processing and sectioning were also more difficult. We realized that sectioning the tooth containing surrounding jaw bone caused more sectioning failure (sample breakage not due to under decalcification) than without the bone. Thus, we decided to remove the jaw bone after decalcification before sample embedment. (3) The crown portion of the tooth was short plus occlusal reduction to prevent tooth fracture causing the lack of space for filling materials unless the entire pulp chamber is filled with fillings. To test regeneration of pulp in the pulp chamber in posterior teeth will be difficult. (4) Due to minimal pulp chamber space to manipulate, the MTA sealing of some cases were not optimal, causing microleakage. Mild inflammation in the pulp was observed in the preliminary studies and formal experiments. Perhaps amalgam filling on top of the MTA and composite bonding is needed to prevent such situation in the future. (5) The root canal morphology was also challenging. The anterior central and lateral incisors are either too long or too large plus curvy to be utilized for the experiment. The second lateral incisors were small and short, which were similar to human maxillary lateral incisor or mandibular incisors, and they were useful for experiments except special care is needed due to tilted long axis of the teeth. Molar teeth were too complex and too posterior to manage and were not suited for our experiments. Premolar teeth starting from second premolar (first premolars were normally too small to operate) to fourth premolar were considered potentially suitable for experiments. Maxillary fourth premolars resemble human first molar but more complex having two palatal roots split at mid-root (Supplementary Fig. S8), therefore they were not quite suitable for experiments. Maxillary third premolars were less difficult, although having three roots made them difficult to operate. Mandibular premolars were more suited for such experiments. Second and third mandibular premolars were relatively easier to handle. Mandibular fourth premolar was manageable with some difficulty, similar to handling human molars. We did not obtain good results from mandibular second premolars due to small pulp chamber space to work with causing ill-filled MTA and composite that created microleakage. An improved work protocol is needed to handle these mandibular premolars for future works.

In the field of endodontics, it has been gradually recognized the impact of pulp-dentin regeneration.[22,23] The most important reasons why we need to develop pulp-dentin

regeneration technology are to restore tooth functions and avoid tooth loss.[22] Because of this recognition, there has been a significant progress in stem cell-based pulp-dentin regeneration research.[23] *De novo* pulp regeneration with additional dentin-like tissue deposition on canal walls can be achieved via stem cell-based approaches either using ectopic mouse models or orthotopic dog models.

In this study, we showed that orthotopic pulp regeneration along with newly generated DB and rD along the canal walls in mini-swine can be achieved. One key problem we observed is that the rD lacks natural dentin structure with organized dentinal tubules. This issue was discussed in our previous review article as to why such organized dentinal tubules are difficult to form in the regeneration process.[24] DPSCs or SCAP are potentially the best cell type to give rise to replacement odontoblasts that would generate dentin. Careful examining the data presented in Figures 2 and 3, we could see dentinal tubules that were formed during the generation of dentin-like mineral next to the HA/TCP granules. The expression of nestin, DSP, DMP1, and BSP in the cells lining against the mineral further suggests the odontoblast phenotype of these cells. The density of the dentinal tubules is not as high as those present in natural dentin, likely due to the irregular shape of the new dentin formed on the HA/TCP. The detectable dentinal tubules are less in the rD formed in the tooth fragment model. As previously discussed,[24] it is likely because of the lack of sufficient number of new odontoblasts formed on the dentinal wall, or the lack of optimal signals to allow proper maturation of odontoblasts.

Oh *et al.* showed that a preameloblast-derived factor, copine 7 (CPNE7), can induce organized dentinal tubule formation in the rD in the tooth fragment mouse model.[25] Without such signaling, bona fide odontoblasts may not be derived or may even be directed into osteoblast-like cells. This phenomenon is more obvious in the orthotopic regeneration. Dentinal tubules that may be observed in the HA/TCP model or tooth fragment model were hardly detected in the orthotopic model (Figs. 6, 7, and 9; Supplementary Fig. S7).

Nonetheless, nestin, DSP, DMP1, and BSP were all detected in the odontoblast-like cells in the regenerated pulp in mini-swine. Although these markers are not odontoblast specific, BSP expression was weak indicating their possible identity of an odontoblast lineage. Providing the right signals to allow DPSCs differentiating into odontoblast lineages appears of critical importance. CPNE7 appeared to enhance odontoblast differentiation thereby producing tubular dentin,[25] therefore, such approach may be tested in the mini-swine model in the future.

Using allogeneic cell sources for pulp-dentin regeneration is an important issue for the field, as it would make such therapy more feasible and prevalent. Most cell therapies prefer the use of autologous cells to avoid transplant rejection, however, MSCs including dental stem cells have a special characteristics–immunosuppression, which can suppress the immune rejection from the host and sustain.[26–28] Allogeneic cell source will circumvent problems if autologous cells are not available. Our finding, although preliminary, indicates the possibility that allogeneic DPSCs may be used for pulp regeneration.

In this study, we used heterogeneous population of DPSCs for regeneration. We did not observe over production of rD that eventually occluded the pulp space. The heterogeneous DPSCs from dog tend to over produce osteodentin and occlude the pulp space,[3] therefore not suited for such purpose. A dog DPSC subset, mobilized DPSCs (MDPSCs), showed ability to completely regenerate pulp after transplantation into the pulpectomized canals in dogs without over producing rD.[4] This also indicates the importance of using multiple large animal studies for pulp regeneration.

There are still many challenges ahead that need to be overcome regarding pulp regeneration, including effective disinfection of the root canal system to increase success of regeneration[29,30] and managing multi-rooted posterior teeth having small apical foramen. The quality of regenerated pulp-dentin complex is another issue that requires further investigation.[24] Additionally, optimal scaffold types require further testing. PLG handled in our experimental protocol appears not suitable for pulp regeneration. While HyA gel is already clinically approved, its longer biodegrading time may slow down the pulp tissue regeneration. Although ColTE has not been clinically approved, the similar product atelocollagen (Koken, Tokyo, Japan)[31] is clinical-grade and may be a suitable option for pulp regeneration.

Our established large animal models can be used to address above-mentioned challenges. Along with more established dog model for pulp regeneration, both models will provide more information to help establish optimal protocols for future clinical use.

Authors' Contributions

X.Z. designed and performed major part of the experimental work, acquired, assembled, analyzed the data, and drafted/revised the article. J.L., Z.Y., and A.A.A. performed part of experiments, analyzed, interpreted the data, and wrote/revised part of the article. C.A.C. and H.A. performed some of the experimental work, assembled the data, and drafted/revised part of the article. G.T.J.H. conceived, designed, performed experimental works and supervised the overall project, analyzed and interpreted the data, and finalized the article. All authors have read and approved the article for publication.

Acknowledgments

The authors thank Dr. Songtao Shi (University of Pennsylvania) for his input during the early developmental stage of the project; Dr. Domenico Ricucci (private practice, Rome, Italy) for his assistance in part of the histology work; Dr. Lonnie D. Shea (Northwestern University) for providing PLG scaffolds; Dr. Mey Al-Habib (Boston University) for initial assistance in testing human tooth fragment model; Dr. Jinsong Huang (UTHSC) for assistance in acquiring micro-CT images; Dr. David Hamilton's team (UTHSC) for assisting general anesthesia and caring of the mini-swine; Drs. Ikbale El Ayachi, Wenhao Zhu, and Jun Zhang (all UTHSC) for their assistance in the mini-swine operations and/or cell isolation. This work was supported in part by a grant from the National Institutes of Health R01 DE019156 (G.T.-J.H.) and a research fund from the University of Tennessee Health Science Center.

Disclosure Statement

No competing financial interests exist.

References

1. Cordeiro, M.M., Dong, Z., Kaneko, T., *et al.* Dental pulp tissue engineering with stem cells from exfoliated deciduous teeth. J Endod **34,** 962, 2008.
2. Huang, G.T.J., Yamaza, T., Shea, L.D., *et al.* Stem/progenitor cell–mediated de novo regeneration of dental pulp with newly deposited continuous layer of dentin in an in vivo model. Tissue Eng Part A **16,** 605, 2009.
3. Iohara, K., Imabayashi, K., Ishizaka, R., *et al.* Complete pulp regeneration after pulpectomy by transplantation of CD105+ stem cells with stromal cell-derived factor-1. Tissue Eng Part A **17,** 1911, 2011.
4. Iohara, K., Murakami, M., Takeuchi, N., *et al.* A novel combinatorial therapy with pulp stem cells and granulocyte colony-stimulating factor for total pulp regeneration. Stem Cells Transl Med **2,** 521, 2013.
5. Ishizaka, R., Hayashi, Y., Iohara, K., *et al.* Stimulation of angiogenesis, neurogenesis and regeneration by side population cells from dental pulp. Biomaterials **34,** 1888, 2013.
6. Zhu, W., Zhu, X., Huang, G.T., Cheung, G.S., Dissanayaka, W.L., and Zhang, C. Regeneration of dental pulp tissue in immature teeth with apical periodontitis using platelet-rich plasma and dental pulp cells. Int Endod J **46,** 962, 2013.
7. Zhu, X., Zhang, C., Huang, G.T., Cheung, G.S., Dissanayaka, W.L., and Zhu, W. Transplantation of dental pulp stem cells and platelet-rich plasma for pulp regeneration. J Endod **38,** 1604, 2012.
8. Zhu, X., Wang, Y., Liu, Y., Huang, G.T., and Zhang, C. Immunohistochemical and histochemical analysis of newly formed tissues in root canal space transplanted with dental pulp stem cells plus platelet-rich plasma. J Endod **40,** 1573, 2014.
9. Bode, G., Clausing, P., Gervais, F., *et al.* The utility of the minipig as an animal model in regulatory toxicology. J Pharmacol Toxicol Methods **62,** 196, 2010.
10. Luo, Y., Lin, L., Bolund, L., Jensen, T.G., and Sorensen, C.B. Genetically modified pigs for biomedical research. J Inherit Metab Dis **35,** 695, 2012.
11. Weaver, M.E., Sorenson, F.M., and Jump, E.B. The miniature pig as an experimental animal in dental research. Arch Oral Biol **7,** 17, 1962.
12. Wang, S., Liu, Y., Fang, D., and Shi, S. The miniature pig: a useful large animal model for dental and orofacial research. Oral Dis **13,** 530, 2007.
13. Stembirek, J., Kyllar, M., Putnova, I., Stehlik, L., and Buchtova, M. The pig as an experimental model for clinical craniofacial research. Lab Anim **46,** 269, 2012.
14. Tziafas, D., Kodonas, K., Gogos, C., Tziafa, C., and Papadimitriou, S. Dentine-pulp tissue engineering in miniature swine teeth by set calcium silicate containing bioactive molecules. Arch Oral Biol **73,** 230, 2017.
15. Tziafa, C., Koliniotou-Koumpia, E., Papadimitriou, S., and Tziafas, D. Dentinogenic activity of biodentine in deep cavities of miniature swine teeth. J Endod **41,** 1161, 2015.
16. Zheng, Y., Liu, Y., Zhang, C.M., *et al.* Stem cells from deciduous tooth repair mandibular defect in swine. J Dent Res **88,** 249, 2009.
17. Zheng, Y., Wang, X.Y., Wang, Y.M., *et al.* Dentin regeneration using deciduous pulp stem/progenitor cells. J Dent Res **91,** 676, 2012.
18. Oguntebi, B., Clark, A., and Wilson, J. Pulp capping with Bioglass and autologous demineralized dentin in miniature swine. J Dent Res **72,** 484, 1993.
19. Alongi, D.J., Yamaza, T., Song, Y., *et al.* Stem/progenitor cells from inflamed human dental pulp retain tissue regeneration potential. Regen Med **5,** 617, 2010.
20. Gauthier, P., Yu, Z., Tran, Q.T., Bhatti, F.U., Zhu, X., and Huang, G.T. Cementogenic genes in human periodontal ligament stem cells are downregulated in response to osteogenic stimulation while upregulated by vitamin C treatment. Cell Tissue Res **368,** 79, 2017.
21. Liao, J., Al Shahrani, M., Al-Habib, M., Tanaka, T., and Huang, G.T. Cells isolated from inflamed periapical tissue express mesenchymal stem cell markers and are highly osteogenic. J Endod **37,** 1217, 2011.
22. Huang, G.T. Dental pulp and dentin tissue engineering and regeneration: advancement and challenge. Front Biosci (Elite Ed) **3,** 788, 2011.
23. Nakashima, M., and Huang, G.T.-J. Pulp and dentin regeneration. In: Huang G.T.-J., Thesleff I., eds. Stem Cells in Craniofacial Development and Regeneration. 1st ed. Hoboken, New Jersey: Wiley-Blackwell, 2013, p. 461.
24. Huang, G.T., and Garcia-Godoy, F. Missing concepts in de novo pulp regeneration. J Dent Res **93,** 717, 2014.
25. Oh, H.J., Choung, H.W., Lee, H.K., *et al.* CPNE7, a preameloblast-derived factor, regulates odontoblastic differentiation of mesenchymal stem cells. Biomaterials **37,** 208, 2015.
26. Wang, L., Morsczeck, C., Gronthos, S., and Shi, S. Regulation and differentiation potential of dental mesenchymal stem cells. In: Huang G.T.-J., Thesleff I., eds. Stem Cells in Craniofacial Development and Regeneration. 1st ed. Hoboken, New Jersey: Wiley-Blackwell, 2013.
27. Zhao, S., Wehner, R., Bornhauser, M., Wassmuth, R., Bachmann, M., and Schmitz, M. Immunomodulatory properties of mesenchymal stromal cells and their therapeutic consequences for immune-mediated disorders. Stem Cells Dev **19,** 607, 2010.
28. Yamaza, T., Kentaro, A., Chen, C., *et al.* Immunomodulatory properties of stem cells from human exfoliated deciduous teeth. Stem Cell Res Ther **1,** 5, 2010.
29. Verma, P., Nosrat, A., Kim, J.R., *et al.* Effect of residual bacteria on the outcome of pulp regeneration in vivo. J Dent Res **96,** 100, 2017.
30. Lin, L.M., Ricucci, D., and Huang, G.T. Regeneration of the dentine-pulp complex with revitalization/revascularization therapy: challenges and hopes. Int Endod J **47,** 713, 2014.
31. Nakashima, M., Iohara, K., Murakami, M., *et al.* Pulp regeneration by transplantation of dental pulp stem cells in pulpitis: a pilot clinical study. Stem Cell Res Ther **8,** 61, 2017.

Address correspondence to:
George T.-J. Huang, DDS, MSD, DSc
Department of Bioscience Research
College of Dentistry
University of Tennessee Health Science Center
875 Union Avenue
Memphis, TN 38163

E-mail: gtjhuang@uthsc.edu

Received: July 25, 2017
Accepted: October 31, 2017
Online Publication Date: December 27, 2017